Pictorial essay of radiological features of benign intrathoracic masses

Syahminan Suut[1], Zeid Al-Ani[2], Carolyn Allen[3], Prabhakar Rajiah[4], Durr-e-Sabih[5], Abdullah AL-Harbi[6], Hamdan AL-Jahdali[6], Ali Nawaz Khan[1]

[1]Consultant Radiologist, Radiology Department, North Manchester General Hospital, Acute Pennine NHS Trust, Crumpsal, Manchester M8 6RB, [2]Specialist Registrar in Radiology, North Manchester General Hospital, Delaunays Road M8 5RB, Manchester, [3]Clinical Director, Acute Pennine NHS Trust, Crumpsal, Manchester M8 6RB, United Kingdom, [4]Assistant Professor, Cardiothoracic Imaging, Radiology Department, Case Western Reserve University, University Hospitals of Cleveland, Cleveland, Ohio, United States, [5]Director, Multan Institute of Nuclear Medicine and Radiotherapy, Nishtar Hospital, Multan 60000, Pakistan, [6]Assistant Professor, Pulmonary Division, King Saud University for Health Sciences, King Abdulaziz Medical City, Riyadh, Saudi Arabia

Address for correspondence:
Prof. Ali Nawaz Khan, North Manchester General Hospital M8 5RB, United Kingdom.
E-mail: drkhan1966@msn.com

Submission: 10-12-2014
Accepted: 30-04-2015

Access this article online

Quick Response Code:

Website: www.thoracicmedicine.org

DOI: 10.4103/1817-1737.160365

Abstract:

With increased exposure of patients to routine imaging, incidental benign intrathoracic masses are frequently recognized. Most have classical imaging features, which are pathognomonic for their benignity. The aim of this pictorial review is to educate the reader of radiological features of several types of intrathoracic masses. The masses are categorized based on their location/origin and are grouped into parenchymal, pleural, mediastinal, or bronchial. Thoracic wall masses that invade the thorax such as neurofibromas and lipomas are included as they may mimic intrathoracic masses. All examples are illustrated and include pulmonary hamartoma, pleural fibroma, sarcoidosis, bronchial carcinoid, and bronchoceles together with a variety of mediastinal cysts on plain radiographs, computed tomography (CT) and magnetic resonance imaging (MRI). Sometimes a multimodality approach would be needed to confirm the diagnosis in atypical cases. The study would include the incorporation of radionuclide studies and relevant discussion in a multidisciplinary setting.

Key words:

Intrathoracic masses, pulmonary mass, radiology

In this modern age of radiology practice, the advent of rapid scanners and quick scan turnover has meant that radiologists encounter a wide spectrum of pathologies.

In the case of thoracic imaging, for example, this would mean that the detection of pulmonary nodules (whether benign or malignant) on thin-section computed tomography (CT) examinations would have become an important part of the daily tasks of many radiologists — both thoracic and general radiologists.[1] CT has predominantly been the imaging technique of choice because certain CT features would help differentiate benign from malignant processes.[2] Difficult areas of interpretation would undoubtedly arise, for example, when assessing for pleural disease. The problem is of global significance, which causes significant morbidity and mortality. Complex imaging with CT, magnetic resonance imaging (MRI), and positron emission tomography-CT (PET-CT) are commonly utilized to allow accurate diagnosis through guided biopsies or even predict prognosis.[3]

Lung carcinoma is obviously the biggest concern, and radiologists play an extremely important role in its detection on imaging. In the last decade, PET-CT has been increasingly employed to improve the assessment of patients with pulmonary nodules. The basis of this is that cells in a malignant tumor undergo glycolysis at an increased rate, and hence have a greater cellular uptake of glucose.[4,5]

The knowledge and ability to confidently interpret benign masses is critical to avoid further unnecessary tests. A number of features are reliable predictors of benignity.[6] High specificity features of benign nodules include calcification (diffuse, popcorn, central, and laminated), internal fat, polygonal (all surfaces concave or straight) unless in contact with a pleural surface, ovoid/flat/tubular shaped and finally clustering of subcentimeter nodules in isolated lung segments.

In addition, a variety of systemic diseases may involve the thoracic structures and it is, therefore, critical for radiologists to be familiar with various patterns of abnormalities associated with them. Even when imaging findings are nonspecific, the radiologist is often the first to suggest the possibilities of diseases when confronted with a particular imaging pattern and supporting laboratory data.[7]

However it should be noted that the role of imaging does have its limitations in certain scenarios. Take, for example, in the setting of a patient with rheumatoid arthritis and the development of pulmonary nodules. Rheumatoid nodules are a rare manifestation of lung disease associated with these arthritides, and their emergence and evolution can be variable. The diagnosis of rheumatoid nodules may therefore be suggested; but if these demonstrate atypical features, accurate diagnosis would still require a combination of baseline imaging, serial follow-up imaging, and even histological confirmation.[8]

The differential diagnoses, when considering a benign pulmonary mass, is wide, and the following [Table 1] is presented for ease of categorization.

Table 1: Differential Diagnosis of Benign Intra-Thoracic Masses

Lung Parenchyma	Bronchial
Hamartoma	Carcinoid
Sarcoidosis	Bronchial Cyst
PMF	Bronchocele
Intrapulmonary Lymph Node	Mediastinal
Rheumatoid Nodules	Hydatid cyst
Pulmonary Infarct	Peritracheal Fibrosis
Cavitating Infarct	Retrosternal Goiter
Wegener's granuloma	Sarcoidosis
Pleural	Pericardial Cyst
Fibroma	Thymoma
Fibroma Mimics	Thymic Hyperplasia
Splenosis	Thymic Cyst
Pleural Plaques	Schwannoma
Loculated Pleural Effusion	Extra-Medullary Hemopoiesis
Rounded Atelectasis	Chronic Calcific Hematoma
Pleural Lipoma	

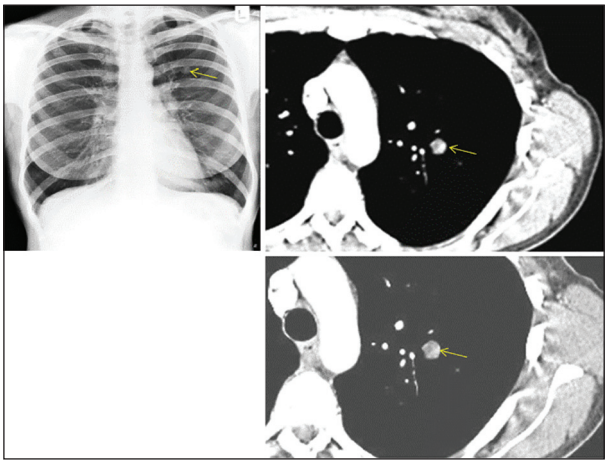

Figure 1: CXR of a 27-year-old female (nonsmoker) showing a solitary well-defined nodule in the left upper zone (arrow). CT further characterizes the opacity by demonstrating fat content within the mass highly suggested of a hamartoma. No biopsy was taken. The nodule remains stable 3 years later. CXR = Chest X-ray, CT = computed tomography

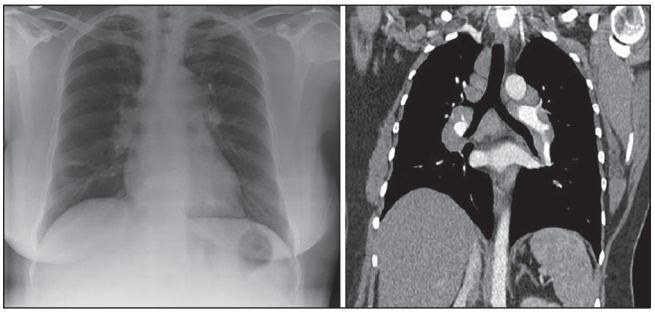

Figure 3: A 35-year-old with known sarcoidosis. Her chest radiograph demonstrates the "Garland sign"—Bilateral hilar and right paratracheal lymphadenopathy. Coronal CT confirms the findings. No lung parenchymal changes are seem

Lung Parenchyma

Hamartoma

As the commonest benign tumor of the lung, pulmonary hamartomas are usually discovered incidentally, but some patients may have hemoptysis or cough. The peak incidence occurs during the 6th decade. They are often detected late and demonstrate slow growth.[9]

Constituting approximately 8% of all lung neoplasms, hamartoma is a tumor which contains cartilage, fat, fibrous tissue, and epithelial components. Malignant transformation is very rare and, therefore, hamartomas are left alone.[10] Characteristically findings on CT include a lesion with a smooth edge, focal fat, or fat alternating with calcific foci (popcorn calcification) [Figures 1 and 2].

Sarcoidosis

Sarcoidosis is a noncaseating, granulomatous, multisystem, chronic, inflammatory condition of unknown etiology. Ninety percent of patients present with lung and mediastinal/hilar lymphadenopathy.[11]

Often patients below the age of 40-years-old are affected and the incident peaks in the 3rd decade of life. Up to half of patients remain asymptomatic, but symptoms would include respiratory complaints such as cough and dyspnea.[11]

CT findings of the chest include paratracheal, mediastinal, and bilateral hilar lymphadenopathy.[12] Pulmonary nodules, if present, would typically be in a peribronchovascular distribution or along fissures [Figures 3 and 4]. Sarcoidosis

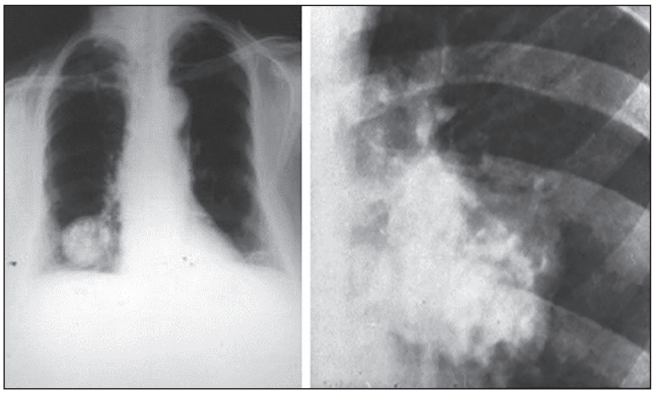

Figure 2: CXRs from two different patients showing the characteristics popcorn calcification of a hamartoma

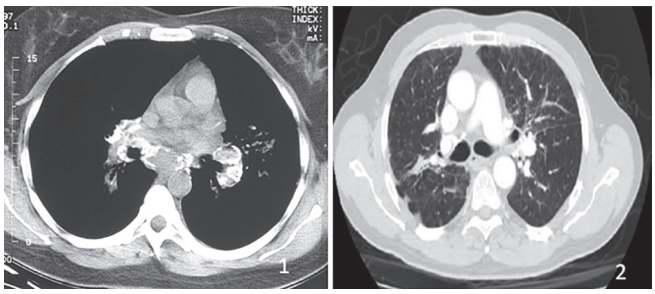

Figure 4: Sarcoidosis in a 56-year-old female patient demonstrating classical eggshell hilar (1) calcification. Note the reticulonodular parenchymal changes of perilymphatic distribution in the middle and upper lobes (2)

can be staged even on the basis of chest radiographs [Table 1].[12]

Progressive massive fibrosis (Pmf)

PMF is also known as complicated silicosis, which develops through the expansion of individual silica nodules. Radiographic findings include large symmetrical bilateral opacities of more than 1 cm, formed by nodule coalescence — typically like angel wings [Figure 5]. CT will confirm the presence of soft tissue masses, which have ill-defined margins and calcifications.[13]

These opacities gradually migrate towards the hilum with evidence of emphysematous changes in the peripheries. The emphysema and volume loss aid the differentiation between unilateral PMF and lung cancer. PMF may be complicated by cavitation, ischemic necrosis, and concomitant tuberculous infection.[14]

Intrapulmonary Lymph Node

Intrapulmonary lymph nodes are commonly detected on CT examination of healthy individuals. Bankoff *et al*., were pioneers of an extensive research performed over a period of 15 years. They discovered that the distribution of intrapulmonary lymph nodes was predominantly in the lower half of the lungs due to larger ventilation and lymphatic fluid production.[15] It is now known that these lymph nodes tend to be oval and occur within a lymphatic distribution subpleurally. They measure approximately 6 mm and can have sharply defined triangular borders [Figure 6]. The nodules are homogeneous and do not calcify.[16]

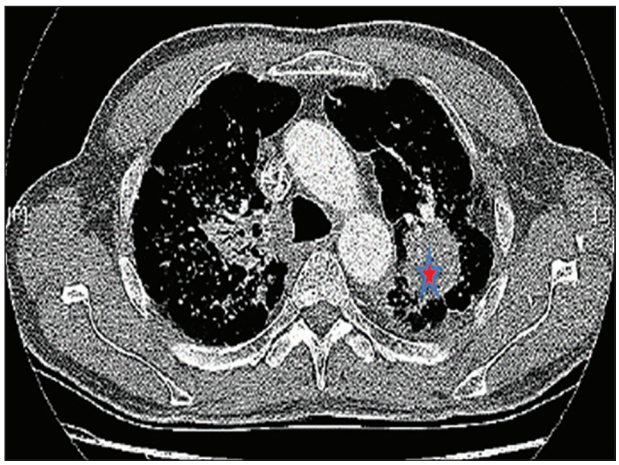

Figure 5: Silicosis massive pulmonary fibrosis (MPF) symmetrical bilateral opacities of more than 1 cm, formed by nodule coalescence forming mass that may even cavitate (*)

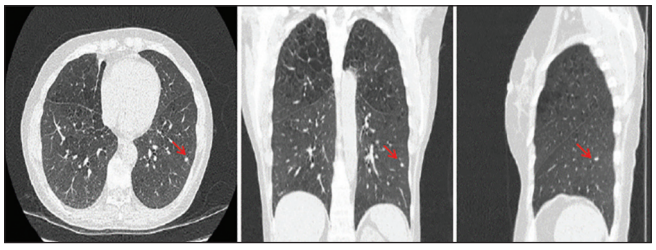

Figure 7: Rheumatoid nodules: Long standing solitary pulmonary nodule in the periphery of the left lower lobe of a 60-year-old male patient with known rheumatoid arthritis. This is likely a rheumatoid nodule

Rheumatoid nodules

The thoracic manifestations of rheumatoid arthritis would include pleural diseases, rheumatoid nodules, diffuse interstitial pneumonia, pulmonary vasculitis, and airway disease. The commonest CT finding according to Tanaka *et al*., was ground glass opacification at 90%. Nodules were observed in 50% of patients and were mostly in the centrilobular distribution. These nodes were thought to arise from antigenic stimuli, for example, from dust inhalation.[17] Figures 7 and 8 are examples of benign rheumatoid nodules.

Pulmonary infarct

Chronic left heart failure and pulmonary embolism are recognized as important causes of pulmonary infarction. The latter can occur despite the dual blood supply to the lungs and the protective effect of the bronchial vasculature. In particular, infarction occurs commonly when vessels less than 3 mm in diameter are occluded.[18,19]

Typical radiographic features include wedge-shaped, pleural-based opacification with no evidence of air bronchograms [Figure 9]. The latter usually occurs in areas of reduced lung attenuation. If there has been recent hemorrhage, the mass will demonstrate a convex border with a halo sign.[18]

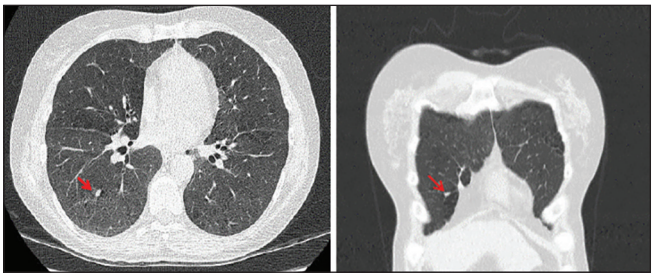

Figure 6: Intrapulmonary lymph node: Incidental finding of a small, oval-shaped parenchymal opacity in the right lower lobe. The appearances are classically those of intrapulmonary lymph node and no further actions are required

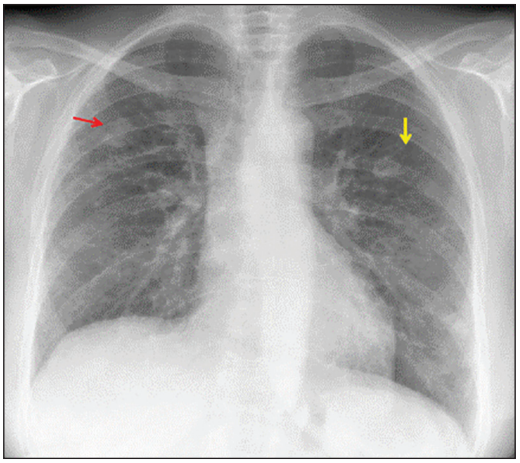

Figure 8: Rheumatoid nodules: PA CXR of a 53-year-old man with seropositive rheumatoid arthritis being treated with rituximab showing a nodule in the right upper lobe (red arrow) and a cavitating nodule (yellow arrow) in the left upper lobe on a background of multinodularity suggestive of Kaplan's syndrome. PA = Posteroanterior

Cavitating infarct

Cavitation, which is associated with pulmonary infarction, is a rare occurrence. These cavities can be aseptic or may be complicated by superadded infection. Wilson *et al*., demonstrated that majority of cavitatory infarction had scalloped inner margins and cross cavity band shadows. Cavitation may occur in septic as well as aseptic emboli [Figures 10-12].[19,20]

Wegener's granulomatosis

Described by Friedrich Wegener, a German pathologist, Wegener granulomatosis is an uncommon disorder, which manifests as chronic granulomatous necrotizing vasculitis involving small- to medium-sized vessels. It is one of the antineutrophil cytoplasmic antibody (ANCA)-associated vasculitides, which affects many organ systems with 90% pulmonary and 80% renal involvement. Classically, patients would present with sinusitis, cough, hemoptysis, and glomerulonephritis.[21]

Lung nodules are the commonest manifestation of Wegner's, and these are multiple and bilateral with no zonal predilection. These measures usually between 2 and 4 cm, and approximately a quarter of those larger than 2 cm may show thin/thick and nodular cavitation [Figure 13]. Wegener's can easily mimic tuberculosis, metastases, lung abscesses, or septic infarcts. If hemorrhage has occurred around nodules, this will manifest as a halo sign, whereby there is ground-glass opacity surrounding a consolidated nodule. Correlation with cytoplasmic antineutrophil cytoplasmic antibodies (c-ANCA) levels may help with the diagnosis.[22]

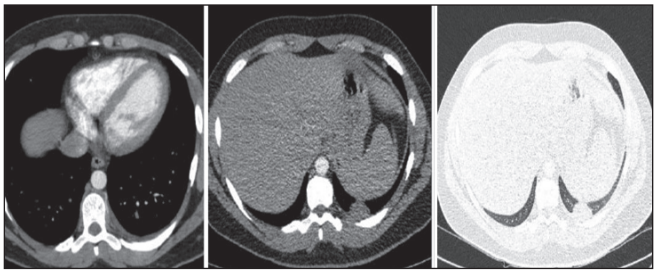

Figure 9: Note the solid pleural-based nodule, associated with a small pleural effusion (pulmonary infarct). The patient had a travel-related deep venous thrombosis that presented with pleuritic, left-sided chest pain

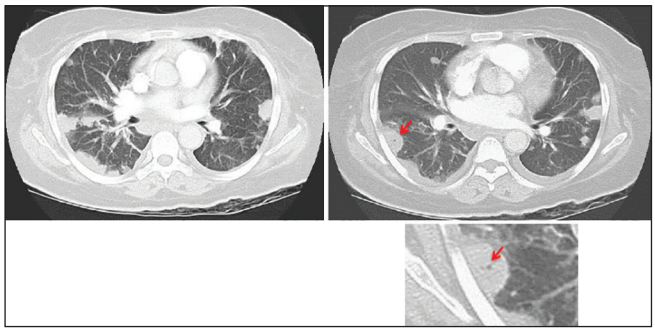

Figure 11: Axial CT images from the same patient as in Figure 10 with a gas gangrene of the foot showing multiple, pleural-based nodules due to septic emboli with evidence of early cavitation in one of the nodules (arrow)

Pleural

Fibroma

First described in 1931, localized or solitary fibrous tumor of the pleura (LFTP) is a rare and slow-growing neoplasm. They are usually discovered incidentally on chest radiographs of asymptomatic individuals. There is no gender predilection or association with prior asbestos exposure. Symptoms would be nonspecific and include cough, dyspnea, chest pain, and hypertrophic pulmonary osteoarthropathy.[11]

LFTPs can be rounded, oblong, or lobulated. They are often found in the dependent portions of the thorax, and if large, they will displace rather than invade adjacent structures [Figure 14]. On unenhanced CT, LFTP would be of soft-tissue attenuation and MR would show intermediate to low signal on T1 and also T2 hypointensity [Figure 15]. Marked enhancement is demonstrated with contrast because of rich vascular supply. There might be associated cysts and hemorrhagic necrosis. Surgical excision is usually curative with a 16% risk of local

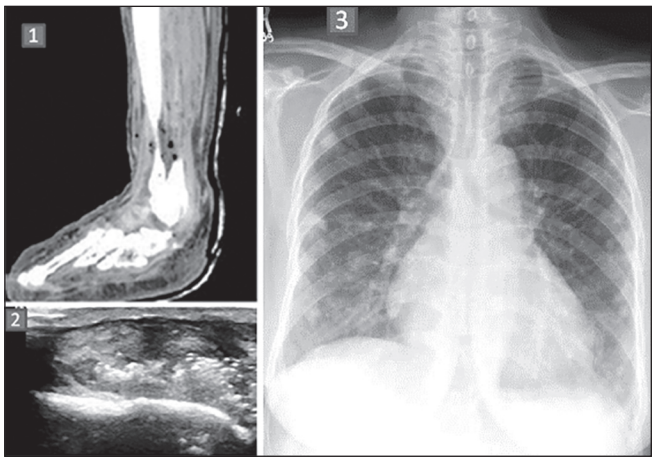

Figure 10: Septic emboli. Gas gangrene of the foot in a 49-year-old woman with type II diabetes mellitus, showing gas within the soft tissues of the foot (1), also elegantly shown by gas within the soft tissues of the foot on ultrasound examination. There are multiple pleural-based nodules on the CXR suggestive of septic emboli (3)

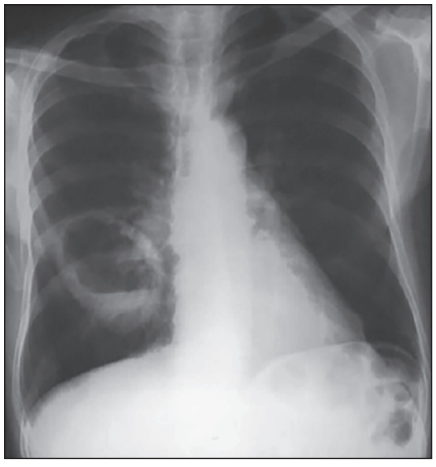

Figure 12: CXR showing a thick-walled cavity with an air-fluid level due to a cavitating pulmonary infarct. The cavity is indistinguishable from other cavities such as cavitating neoplasia. To achieve a diagnosis, the history and the radiological evolution is important. This patient was a known pulmonary infarct, which subsequently cavitated

recurrence.[23] Fibroma mimics, would include mesothelioma, pleural lipoma, pleural fibrosarcoma, or intercostal nerve neurilemoma (schwannoma).[23]

Splenosis

Intrathoracic splenosis is rare and involves autotransplantation of splenic tissue into the pleural cavity, commonly secondary to diaphragmatic and splenic rupture following blunt or penetrating abdominal trauma [Figure 16]. Thourani *et al*., described the chest radiographic findings of a pleural-based mass (confirmed on CT). Surgically they observed numerous purplish implants throughout the thoracic cavity which covered the pleural, pericardial, and hemidiaphragmatic surfaces. The presence of Howell-Jolly bodies on postoperative blood smear confirmed the diagnosis of intrathoracic splenosis.[24]

Intrathoracic splenosis is usually a benign condition, in comparison to abdominal splenosis whereby patients may present with pain and bowel obstruction. Imaging diagnosis can be made by technetium 99m Tc-labeled heat-damaged erythrocyte scan, 99mTc sulfur colloid scintigraphy, or indium 111 In-labeled platelet scan [Figure 17].[24,25]

Pleural Plaques

Pleural plaques are the commonest manifestation of asbestos exposure, which usually arise from the parietal pleura, but can also involve visceral pleura [Figure 18]. There is usually a latency period of 20-30 years. Classically, pleural plaques on chest radiographs are seen along the posterolateral chest wall and features are pathognomonic when seen along the dome of the diaphragm. The costophrenic angles and apices

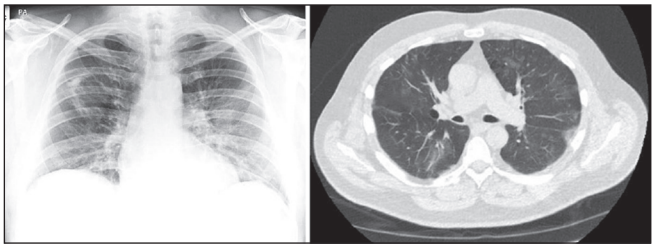

Figure 13: Wegener's granulomatosis: CXR in a patient with Wegener's granulomatosis showing a thick-walled cavity in the left upper lobe and patchy bilateral basal shadowing. CT confirmed multiple ground glass changes in keeping with pulmonary hemorrhage secondary to the disease

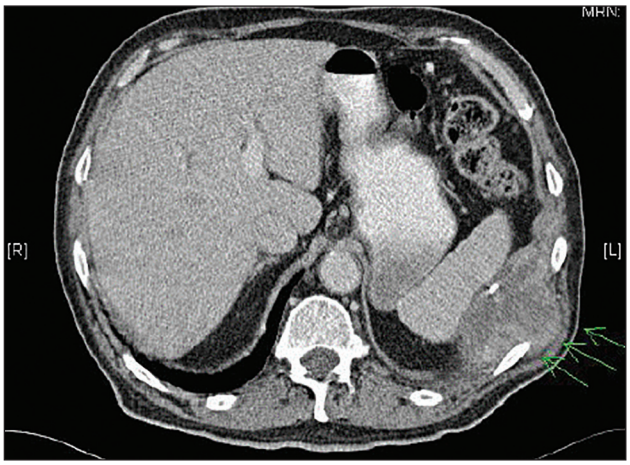

Figure 15: A pleural fibroma should not be confused with a mesothelioma, note the calcified pleural plaque, a pleural-based mass invading the intercostal space (arrow) in this patient with previous asbestos exposure

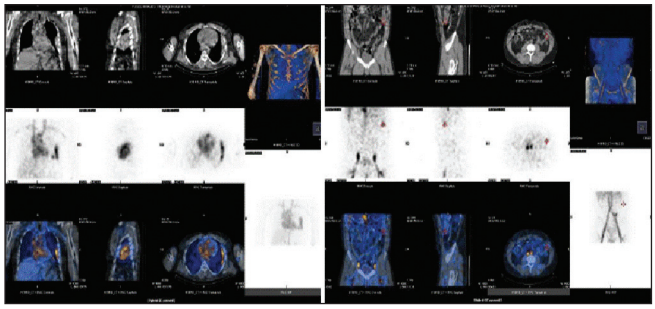

Figure 17: Splenic scintigraphy SPECT/CT study scans confirm intense uptake in the left hemithorax pleural nodularities. The appearances are those of post-traumatic abdominal and intrathoracic splenosis. SPECT = Single-photon emission CT

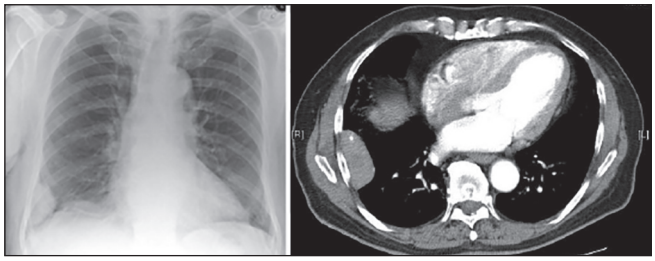

Figure 14: Pleural fibroma: Incidental pleural-based mass in the right costophrenic angle in a 65-year-old male presenting with shortness of breath. CT confirms the presence of a well-defined homogenous right lower parietal pleural mass measuring 6 cm × 3 cm with focal calcification

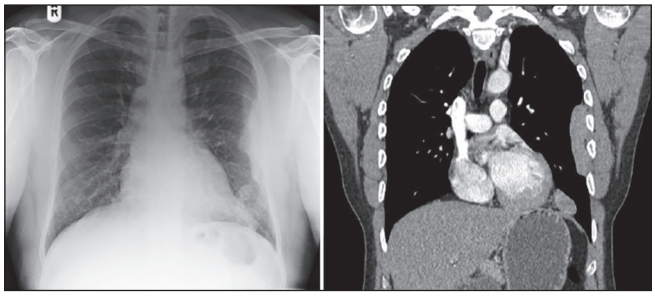

Figure 16: Splenosis: Incidental finding on a chest radiograph of a left-sided, pleural-based mass. CT confirms this and also other pleural nodularities, with the absence of a spleen. Further history was obtained and this patient was noted to have been involved in a blast injury. Splenic injuries were therefore suspected

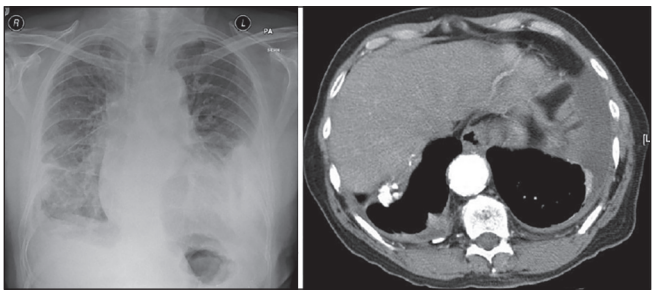

Figure 18: Soft and calcified pleural plaques, due to asbestos exposures. Soft plaques cannot be reliably differentiated from a mesothelioma without a biopsy

are usually spared. Calcification of these plaques occurs in 10-15% of case.[26,27]

Asbestosis rarely occurs in the absence of pleural plaques. In fact, pleural effusion is the earliest manifestation of previous asbestos exposure and this usually has a latency period of 10 years.[27]

Loculated Pleural Effusion

Feldman in 1951 has described localized interlobar pleural effusion as a reversible entity and typically occurred during congestive heart failure. The effusion can either clear spontaneously or with treatment response. The disease thought to provoke this response was termed obliterative pleuritis.[28]

A loculated interlobular pleural effusion or pulmonary pseudotumor is a term frequently used to describe focal fluid collections trapped in the pleural fissures. Particularly on chest radiographs, these entities can cause confusion and appear as a solid pulmonary mass [Figures 19 and 20]. The opacities are typically elongated along the direction of the fissures and may have tapered ends. A lateral chest radiograph is often useful for further characterization these masses. In equivocal cases, CT would help establish the fluid density of the apparent mass and its location within a minor or major fissure[Figure 19].[29]

These vanishing tumors are often seen in patients presenting with congestive cardiac failure. As the patient's disease begins to improve, radiological features would sometimes lag and the resorption of the interlobar pleural fluid would be slower to show resolution than the other signs of cardiac failure. An eventual chest radiograph would however show resolution of the fluid.[28-30]

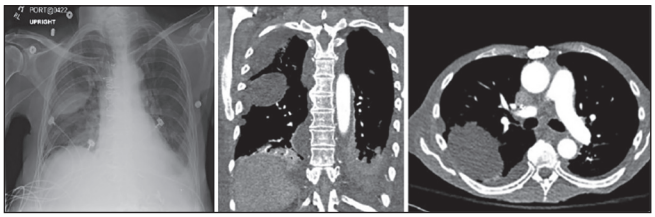

Figure 19: Loculated interlobular pleural effusion or pulmonary pseudotumor; also called vanishing tumor

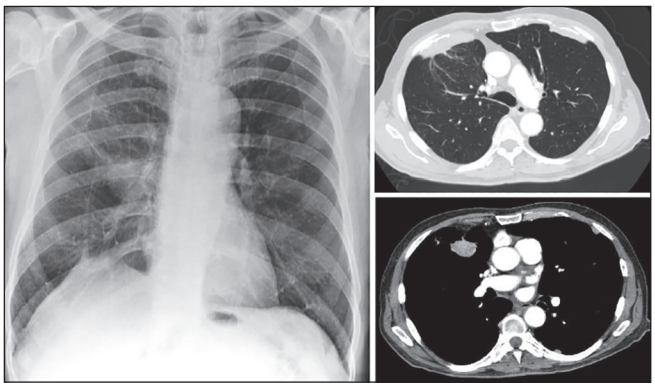

Figure 21: Round atelectasis occurs when there is unfolding of redundant pleura. This may give a false, mass-like appearance. It is most commonly associated with asbestos-related disease, but it may arise from a variety of chronic pleural conditions such as infection, uraemia, therapeutic pneumothorax in the treatment of tuberculosis, pulmonary infarction, or heart failure and is usually asymptomatic. The images show a rounded atelectasis in association with pleural thickening secondary to asbestoses exposure

Rounded Atelectasis

Round atelectasis may mimic a pulmonary mass lesion. It is an unusual form of lung collapse or folded lung, which lies adjacent to the pleural surface. Hanke and Kretzschmar coined the term round atelectasis, and this entity affect predominantly male patients and those with prior asbestos exposure.[31] It is almost always asymptomatic and is typically detected incidentally on chest radiographs.[32]

Characteristically, round atelectasis demonstrate the comet tail sign. Commonly seen in the posterior aspect of a lower lobe, bronchi and vessels curve into an apparent mass at its hilar pole—this feature is important to recognize. The adjacent pleural thickening is an essential feature [Figure 21]. The affected lobe would demonstrate volume loss and the mass may have air bronchograms.[32,33]

No specific treatment is required for round atelectasis. They will be slow growing, remain stable, or spontaneously disappear. Fine-needle aspiration biopsy is however required in equivocal cases, to distinguish this entity from bronchogenic carcinomas.[32]

Pleural Lipoma

The commonest benign soft tissue of the pleura is a pleural lipoma. These soft, fatty, and encapsulated tumors are slow growing and originate from the submesothelial layers of the parietal pleura and may extend into the subpleural/pleural/extrapleural space [Figure 22]. They can become extremely large. Patients would often remain asymptomatic or present with nonproductive cough, exertional dyspnea, chest heaviness,

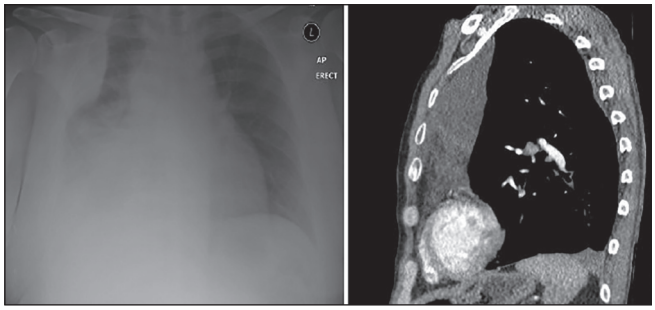

Figure 20: Loculated pleural effusion: A smoothly-defined, right, pleural-based mass is demonstrated on the chest radiograph. On CT, this "mass" was noted to be of fluid density. Appearances are in keeping with a loculated pleural effusion

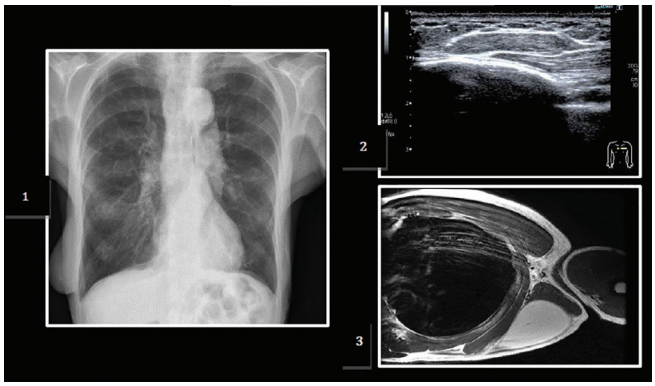

Figure 22: Chest wall lipoma: Examples of chest wall lipomas on differing imaging modalities. The chest radiograph (1) demonstrates a well-defined, smooth, right lateral chest wall mass. Ultasound scan (2) demonstrates a homogeneous mildly echogenic ovoid structure and T1-weighted MR scan (3) demonstrated a homogeneous. MR = Magnetic resonance

or back pain. Radiographic features include fat attenuation and homogeneity on CT (approximately HU-100).[10]

Molinari *et al*., describes the importance of differentiation of a pleural lipoma from a liposarcoma. Liposarcomas may arise in all thoracic regions which contain adipose tissue. The inhomogeneity of these tumors on either CT or MRI helps differentiate liposarcomas from lipomas. Irregular areas of enhancing soft tissue would also suggest a malignant nature. If in doubt, 18-fluorodeoxygenase positron emission tomography (18-FDG-PET) may be valuable in the differentiation of lipomas from liposarcomas.[34]

Bronchial

Carcinoid

These are uncommon pulmonary neoplasms of neuroendocrine origin. Approximately 75% of bronchial carcinoid tumors arise in the lobar bronchi, 10% occur in the main-stem bronchi, and 15% originates in the periphery of the lung. They secrete a variety of chemical substances, but association with carcinoid syndrome is very rare. Occasionally, Cushing's syndrome due to ectopic hormone production is caused by bronchial carcinoid tumors.[35]

Seventy-five percent of bronchial carcinoids are detected on conventional chest radiographs with smaller ones only seen on CT.[35] Radiologic findings are usually related to bronchial obstruction. Central bronchial carcinoids manifest as a well-defined endobronchial nodule, hilar or a perihilar mass closely related to the bronchial tree. Associated atelectasis, air trapping, obstructing pneumonitis, and mucoid impaction may also be seen. Peripheral bronchial carcinoids appear as solitary nodules [Figure 23]. Calcification is common and is easily visualized at CT.[36]

Prognosis of bronchial carcinoids is highly dependent on histologic findings and stage of the tumor: Typical bronchial carcinoids have an excellent prognosis, whereas atypical bronchial carcinoids have a worse prognosis.[35,36]

Pulmonary resection is the treatment of choice for bronchial carcinoids.[36]

Bronchogenic cysts

Is a rare congenital malformation of the bronchial tree; however, it is considered the commonest of foregut duplication cysts. It accounts for 5-10% of pediatric mediastinal masses. Most bronchogenic cysts are asymptomatic and found incidentally on imaging. However, mediastinal cysts can present as a mediastinal mass that may enlarge and cause local compression and respiratory distress. Infection of bronchogenic cysts is also reported.[37]

Bronchogenic cyst forms as an abnormal budding of the bronchial tree during embryogenesis that is lined by secretory respiratory epithelium (cuboid or columnar ciliated epithelium). The wall is made up of tissues similar to that of the normal bronchial tree, including cartilage, elastic tissues, mucous glands, and smooth muscle. They contain water, variable amounts of proteinaceous material, blood products, and calcium oxalate; and hence can be confused with solid lesions due to their high attenuation content. They do not usually communicate with the bronchial tree and therefore typically are nonaerated. Occasionally a communication may develop following infection or intervention, resulting in and air-filled cystic structure with an air-fluid level.[38]

Bronchogenic cysts can be classified as mediastinal and intrapulmonary types. The most common location is the middle mediastinum (65-90%). Parenchymal (intrapulmonary) bronchogenic cysts are typically perihilar with lower lobes predilection.[37]

On plain radiographs, the cysts usually appear as soft-tissue density rounded structures, sometimes with compression effect of surrounding structures. On CT, they appear as well-circumscribed spherical or ovoid masses of variable attenuation as discussed above.

Approximately 50% are fluid density (0-20 HU), with the remaining cysts being of soft tissue density (>30 HU) or even hyperdense compared to the mediastinal soft tissue. CT can also detect calcium oxalate (milk of calcium) layering dependently. No solid contrast enhancement is the general rule [Figures 24 and 25].[38]

Treatment options include surgical excision of the cyst considering the chance of developing complications like infection, hemorrhage, bronchial obstruction, and rarely, to undergo

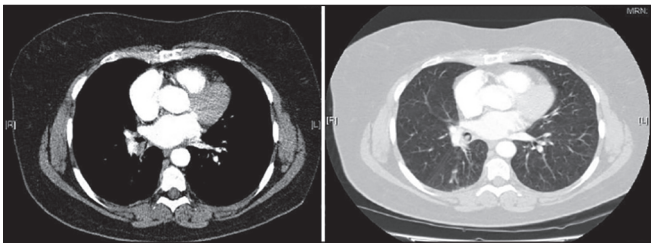

Figure 23: Carcinoid: CT in a breathless 70-year=old gentleman demonstrates the presence of an endobronchial lesion in the right bronchus intermedius. An end-bronchial ultrasound (EBUS) was performed and samples obtained. This was later shown to be a bronchial carcinoid

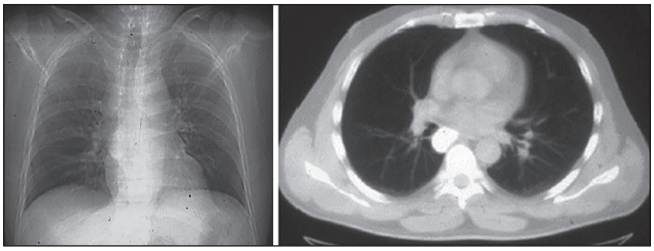

Figure 24: On a CXR bronchogenic cysts usually appear as soft-tissue density rounded structures. As the cysts may contain calcium oxalate, dependent layering of calcific density material may occasionally be seen as seen on the CXR. CT is better able to detect calcium oxalate (milk of calcium) layering dependently as shown

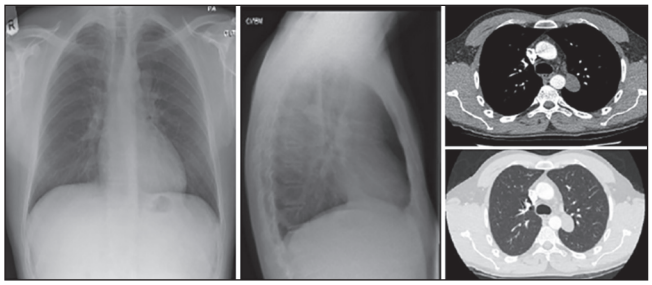

Figure 25: Bronchogenic cyst: Well-defined, left hilar shadows seen on the chest radiograph. CT shows well-defined 3.5 × 24 cm uniformly low attenuation (HU 34) lesion arising from the posterior mediastinum in keeping with a bronchogenic cyst

malignant transformation. Increasingly, these lesions are treated with transbronchial or percutaneous CT-guided aspiration that will confirm the diagnosis and treat/reduce their size. Small lesions can be followed, however, they do have a tendency to increase in size over time, sometimes rapidly.[38] Malignant transformation is very rare, but reported, with primaries including: Rhabdomyosarcoma, pleuropulmonary blastoma, anaplastic carcinoma, leiomyosarcoma, and adenocarcinoma.[39]

Bronchocele

Bronchocele (bronchial mucocele) refers to a mucous-filled and dilated bronchus surrounded by aerated lung.[40] These can be the result of an obstructive lesion to the bronchial tree as in congenital bronchial atresia where they usually affect the apicoposterior segment of the left upper lobe. Other obstructive causes include benign or malignant bronchial neoplasms, bronchogenic cysts, and foreign bodies. Nonobstructive bronchoceles are usually seen in asthmatic patients due to increased mucous production.[41] Asthmatic patients are also predisposed to Aspergillus infection and, therefore, allergic bronchopulmonary aspergillosis (ABPA) can result in bronchocele with a characteristic branching pattern. Cystic fibrosis is also a reported cause of nonobstructive bronchoceles due to impaired ciliary movement and thick secretions.[42]

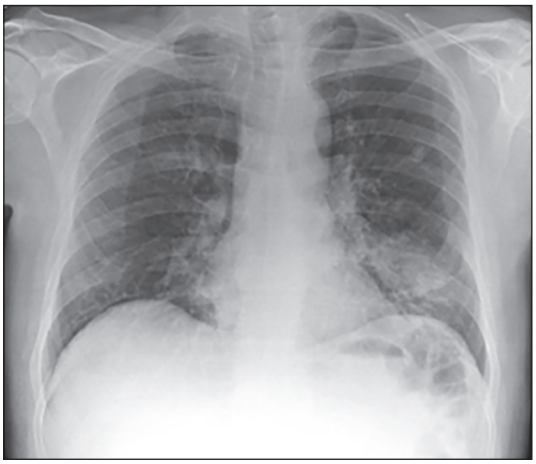

Figure 26: Bronchocele: Chest radiograph performed in asthmatic 50-year-old male demonstrated branching tubular structures in the left lower zone. An incidental left upper zone nodule has remained unchanged for many years

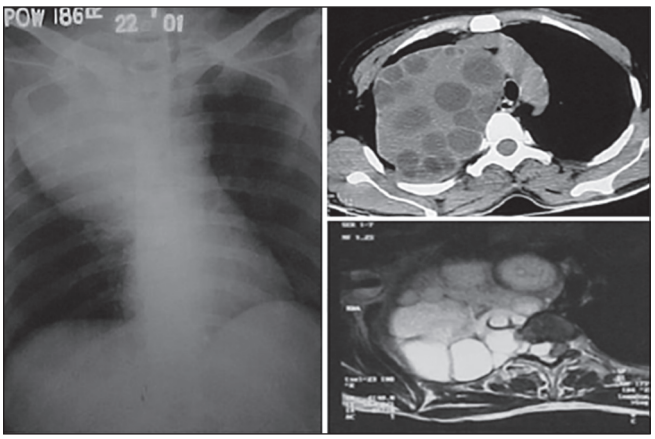

Figure 28: This patient presented with severe right shoulder pain. The CXR and T1- and T2-weighted axial images show features of a hydatid cyst in the right superior sulcus (Images courtesy: Shyam Sunder)

Bronchoceles can be difficult to diagnose on plain radiographs as their branching tubular opacity can be difficult to differentiate from the normal vascular pattern. CT would better define a tubular and branching intrapulmonary opacity that is distinct from vascular shadows [Figures 26 and 27]. Their appearance is sometimes described as a typical "finger in glove". CT attenuation of the mucus can be high in ABPA.[42] The typical appearance for a bronchocoele resulting from bronchial atresia occurs immediately distal to the expected location of the apical segmental bronchus, where there will be a hyperlucent segment or lobe distal to the bronchocele owing to collateral air drift.[41]

Mediastinal

Hydatid cyst

Hydatid cyst disease results from infection by the larval stage of the dog tapeworm *Echinococcosis granulosus*. The lung is the second most common site of involvement with *Echinococcosis granulosus* in adults after the liver. Thoracic involvement may occur by transdiaphragmatic route in cases of hepatic disease or via hematogenous spread.[43]

Chest radiographs and CT are the most widely used modalities to image thoracic hydatid disease. Chest CT features include multiple or solitary cystic lesion [Figure 28]. Size can be variable, ranging between 1 and 20 cm and usually demonstrate lower lobes predilection. Air crescent sign and floating membranes (water lily sign) are described in cases of hydatid cyst ruptures.[44]

Surgery remains the mainstay of treatment. Less invasive methods and combinations with chemotherapy are being developed.

Goiter

Enlargement of the thyroid gland is one of the causes of superior mediastinal mass [Figures 29 and 30]. Although

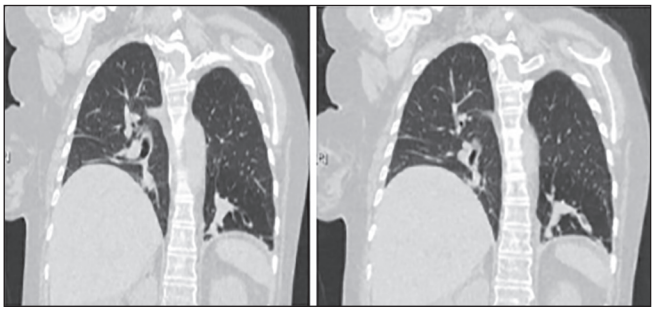

Figure 27: Bronchocele: CT confirms the presence of dilated and ectatic left lower lobe bronchioles with evidence of mucus impaction. Appearances are suggestive of bronchocele secondary to asthma and increased mucus production

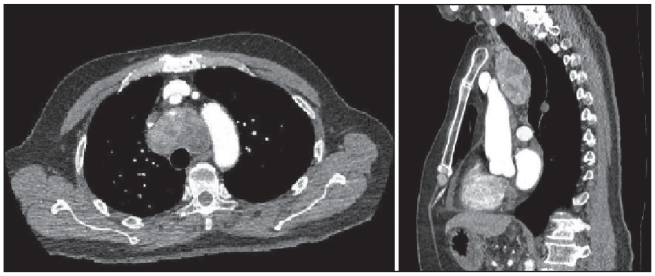

Figure 29: Retrosternal goiter: Axial and sagittal CT images show heterogeneous, well-defined, 6.5 × 24.0 cm, right retrosternal goiter with speckles of calcification

there is no clear definition, but thyroid gland enlargement is considered as a goiter that requires surgical removal when there is retrosternal extension with intrathoracic component appears to extend more than 3 cm from the thoracic inlet [Figure 31].[45]

Ultrasound with Doppler studies is the imaging modality of choice when there is clinical suspicion of enlarged thyroid gland. The latter modality usually demonstrates diffuse enlargement/nodularity of the gland with possible colloid content. It is also useful to evaluate retrosternal extension. CT can evaluate the degree of intrathoracic extension in larger goiters. They usually demonstrate contrast enhancement and may contain calcification.

Pericardial cyst

These are uncommon congenital cysts of the anterior and middle mediastinum that result from abnormalities in the development of the coelomic cavities. Rarely can they occur as a result of previous pericarditis.[46] Most cases are diagnosed incidentally on imaging and remain asymptomatic.

Pericardial cysts are typically seen as right cardiophrenic angle mass, but can be found anywhere adjacent to the heart [Figure 32]. On CT, they appear as well-defined, nonenhancing, low (water) attenuating, rounded mass next to the pericardium. MR examination usually shows typical fluid signal content with occasional high signal on T1-weighted images due to proteinaceous material and there is no enhancement with intravenous contrast on CT or MR [Figure 33].[47]

Thymoma

Thymoma is a rare mediastinal neoplasm, but is the most common primary neoplasm of the anterior mediastinum.[48] They typically present in the 5th-6th decades, without gender predilection. Presentation is usually secondary to mass effect within the anterior mediastinum (venous obstruction, dysphagia, or breathing difficulties secondary to airway's compression). It has strong association with myasthenia gravis, 10-20% of patients with myasthenia gravis have a thymoma, 30-50% of patients with a thymoma have myasthenia gravis. Other associations include pure red cell aplasia, hypogammaglobulinemia, systemic lupus erythematosus (SLE), rheumatoid arthritis, and non-thymic cancers. Thymomas can be divided into invasive and noninvasive ones. The latter tend to be noncapsulated and may show pleural seeding at time of diagnosis. They are usually unresectable and with poor prognosis.[49] Plain films will show a well-defined, lobulated anterior mediastinal mass which can demonstrate associated calcification. CT will show soft tissue attenuation masses usually seen between the sternum and great vessels [Figures 34-36]. Mediastinal lymph node enlargement may be present (13-44%).[50]

Thymic hyperplasia

Thymic hyperplasia refers to hyperplasia of the thymus gland. The latter is important to differentiate from thymic neoplasms. Diffuse and symmetric enlargement of the gland is the most common radiological finding differentiating it from neoplasms, which tend to manifest as focal masses [Figure 36]. Both thymic hyperplasia and malignancy can demonstrate increased activity on FDG-PET because the thymus demonstrates normal physiologic uptake and, therefore, differentiation between the two is difficult.[51]

Pathologically, thymic hyperplasia can be divided into two forms. These cannot be differentiated on the basis of imaging: i- True thymic hyperplasia: This is usually associated with chemotherapy, radiotherapy, and systemic stresses; and

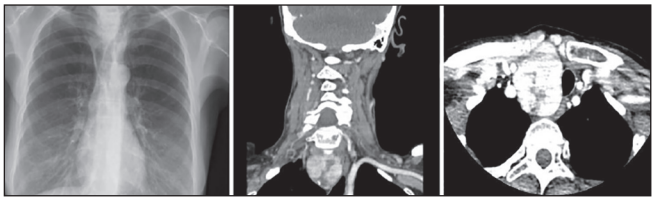

Figure 30: Retrosternal thyroid: Chest radiograph demonstrates a soft tissue mass in the superior right mediastinum causing deviation of the trachea to the contralateral left. CT confirms a heterogeneous 5 cm × 4 cm right retrosternal thyroid gland

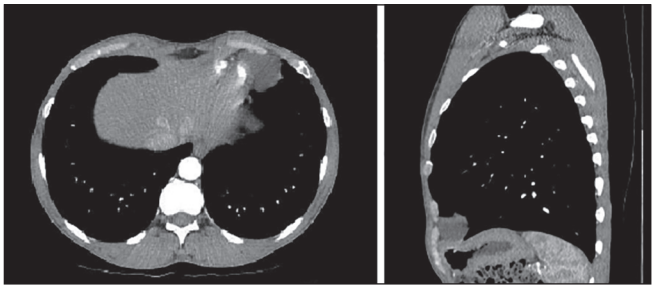

Figure 32: Pericardial cyst: Axial and sagittal views of an arterial contrast-enhanced scan through the thorax of another patient demonstrated a 3.5 cm × 2.0 cm left pericardial cyst in the region of the lingual

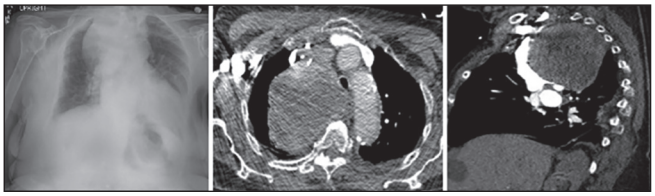

Figure 31: Retrosternal thyroid: CXR demonstrates a large soft tissue mass in the superior right mediastinum causing deviation and compression of the trachea and displacement of the mediastinum to the contralateral left. CT confirms a heterogeneous right retrosternal thyroid gland. The patient presented with stridor at surgery; a partial thyroidectomy confirmed benign retrosternal goiter

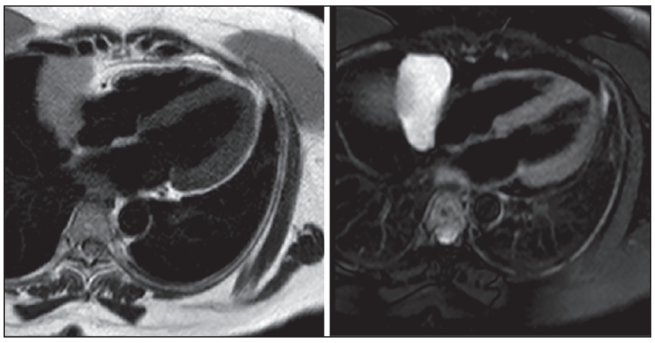

Figure 33: Pericardial cyst: Axial T1- and T2-weighted MRI showing typical fluid signal in the pericardial cyst with occasional high signal on T1-weighted images (not shown). MRI = MR imaging

ii- lymphoid hyperplasia which is usually associated with myasthenia gravis, SLE, rheumatoid arthritis, scleroderma, and Graves' disease.[52]

Thymic cyst

Thymic cysts can be seen in cervical or mediastinal regions. They are usually divided into:

Congenital — often unilocular or acquired - often multilocular and can happen secondary to thoracotomy, chemotherapy, or radiotherapy for mediastinal malignancy or secondary to inflammation.[53] On CT, thymic cysts can be lobulated and may demonstrate soft-tissue attenuation components. They usually show typical cystic signal characteristic on MR without intrinsic enhancement [Figures 37-39].[54]

Schwannoma

Benign nerve sheath tumors are usually seen as posterior mediastinal or paraspinal masses. On CT, schwannomas are frequently heterogeneous with areas of low attenuation secondary to cystic degeneration, hypercellularity, hemorrhage, lipid, or myelin. Punctate calcifications may also be detected on CT [Figure 40].

Enhancement pattern can be variable (homogeneous, heterogeneous, or peripheral). They may extend through the adjacent intervertebral foramen to the spinal canal with a "dumb-bell" configuration. MRI typically exhibits low-to-intermediate signal intensity on T1-weighted imaging and may show areas of intermediate-to-high signal intensity on T2-weighted imaging.[55]

Extramedullary Hematopoiesis

Extramedullary hematopoiesis is a response to erythropoiesis failure in bone marrow. Therefore, this disease can be seen in hemoglobinopathies, myeloproliferative disorders, or bone marrow infiltration. It tends to affect spleen and liver and

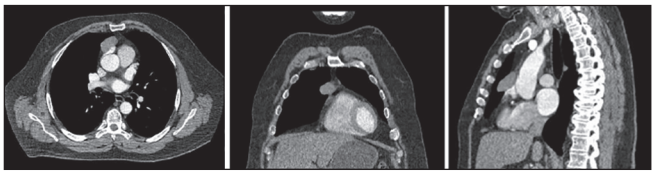

Figure 34: A 45-year-old man recently diagnosed with myasthenia gravis undergoes CT thorax. This demosntrated a 2.5 cm × 3.5 cm, well-defined homogenous anterior mediastinal mass in keeping with a thymoma

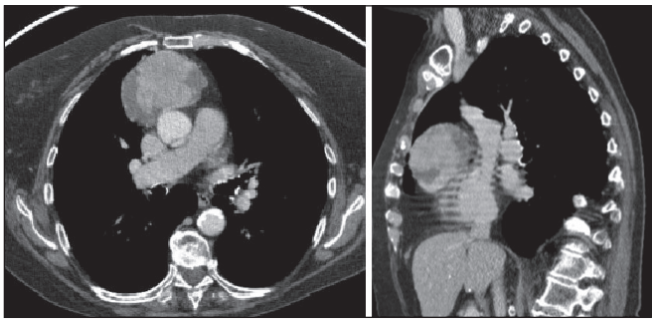

Figure 36: This male patient in the mid-30s presented with clinical features of myasthenia gravis. The axial and sagittal CT showed a mass in the anterior mediastinum, with slight surface tumor irregularity and areas of necrosis. At surgery a malignant thymoma was confirmed

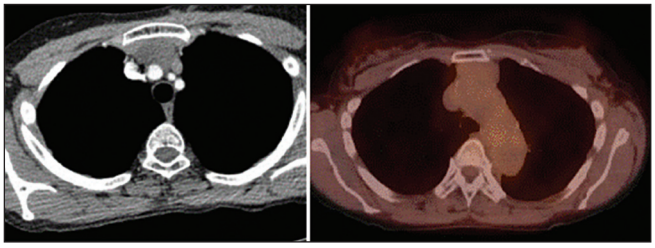

Figure 38: Axial CT through the anterior mediastinum shows a lobulated thymic mass with low attenuation areas in keeping with thymic cysts. FDG-PET shows no uptake within the cysts

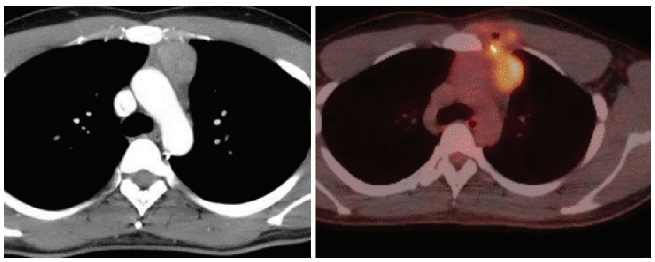

Figure 35: Thymoma: Axial CT shows a well-defined homogenous anterior mediastinal mass in a patient that presented with myasthenia gravis. FDG-PET showing uptake within the tumor. A thymoma was confirmed at surgery. FDG-PET = Fluorodeoxygenase positron emission tomography

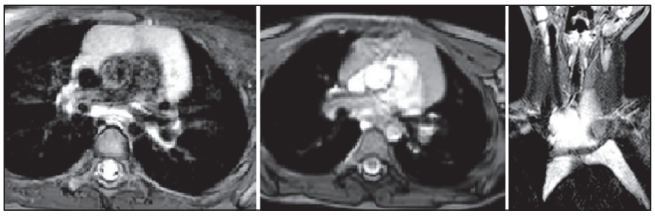

Figure 37: STIR sequence and T2-weighted axial and coronal images through the mid mediastinum showing diffuse symmetric and smooth enlargement of the thymus gland due to thymic hyperplasia. STIR = Short TI inversion recovery

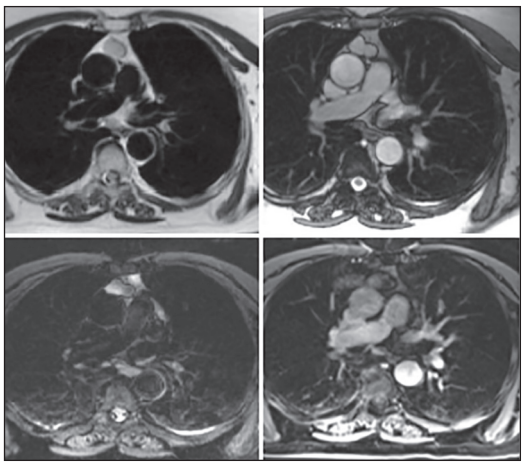

Figure 39: Cystic thymoma: Axial T1, T2, and post-gadolinium MRI showing characteristic features of a cystic thymoma without intrinsic contrast enhancement

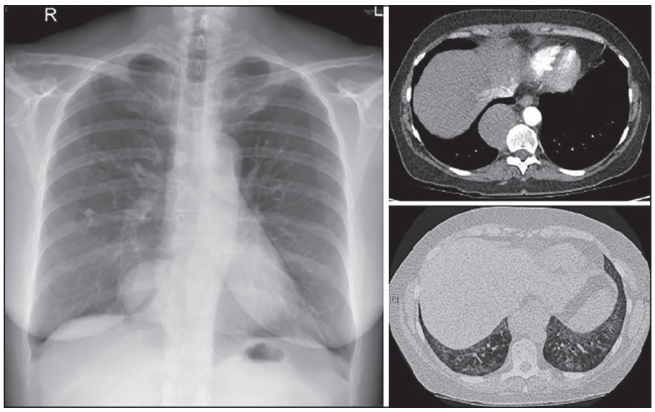

Figure 40: CXR shows a well-defined, smooth, lower right paravertebral mass with close association with spinal canal (axial CT) in keeping with a benign neurogenic tumor

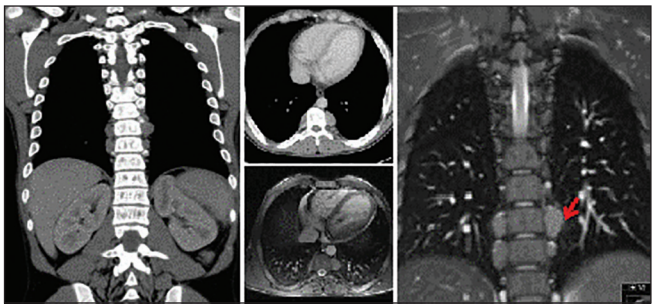

Figure 41: Extramedullary hematopoiesis usually occurs in association with hematological disorders and normally involves the reticuloendothelial system, including the liver, spleen, and lymph nodes. This patient had a beta thalassemia. Note the paravertebral location of the extramedullary hematopoiesis

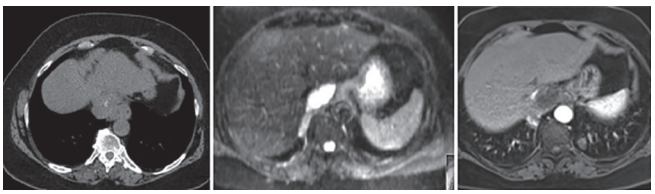

Figure 42: Noncontrast axial CT, T2-weighted MR, and post-contrast CT chest shows features of a chronic calcific hematoma

occasionally in the lymph nodes. Less common organs include the pleura, lungs, gastrointestinal tract, and kidneys.[55]

Radiological manifestation of thoracic disease usually includes paraspinal masses (usually bilateral) with rounded and lobulated margins. Medullary expansion of the bony structures with trabeculae resorption can be seen [Figure 41]. These masses do not calcify or cause bone erosion. They tend to show low attenuation on CT with mild contrast enhancement. Other less common thoracic manifestation of the disease includes interstitial pulmonary abnormality, pleural mass, or hemothorax. Spleen can be enlarged or absent. Diagnosis can be confirmed with percutaneous fine-needle aspiration or biopsy. Usually this condition regresses with treating the underlying cause.[55]

Chronic Calcific Hematoma

Kidner in 1917 noted that calcified hematoma would occur secondary to trauma.[56] He proposed that pathologically, deep muscle fibers would tear after any trauma, and a break in the periosteum would occur at the same time. The resulting hemorrhage would form a mass in the deepest layer of tissue. A fibrous tissue membrane would later form to prepare for blood clot absorption. Eventually, there is calcium deposition.

In the current radiological context, a thoracic chronic expanding hematoma (CEH) presents clinically as a slowly growing mass months or years after the initial injury. Calcified hematomas may grow to a very large size occupying the entire hemithorax with distortion of the mediastinum [Figure 42]. Patients at this stage may present with respiratory distress.[57]

Pathologically, the calcified mass will contain central mass of blood and a wall of granulation tissue, which is dense along the periphery. A CT-guided needle biopsy can be performed to exclude infectious or neoplastic cells. There, however, needs to be care in the diagnostic process due to risk of massive bleeding. Total surgical removal would be the treatment of choice.[57,58]

Conclusion

The overall importance of good radiology detection and clinical judgment cannot be underestimated. If not, there can be implications of misdiagnosis and unnecessary further investigations, which will in turn carry the risk of radiation burden and can, lead to invasive procedures like biopsies. Furthermore there is significant impact on departmental resources and financial costs.

Finally, with reference to this review, good clinicoradiological understanding of benign entities would ensure smooth communication of findings to clinicians and most importantly allay patient worries.

References

1. Leader JK, Warfel TE, Fuhrman CR, Golla SK, Weissfeld JL, Avila RS, *et al*. Pulmonary nodule detection with low-dose CT of the lung: Agreement among radiologists. AJR Am J Roentgenol 2005;185:973-8.
2. Salahudeen HM, Hoey ET, Robertson RJ, Darby MJ. CT appearances of pleural tumours. Clin Radiol 2009;64:918-30.
3. Helm EJ, Matin TN, Gleeson FV. Imaging of the pleura. J Magn Reson Imaging 2010;32:1275-86.
4. Gill RS, Perry T, Abele JT, Bedard EL, Schiller D. The clinical significance of incidental intra-abdominal findings on positron emission tomography performed to investigate pulmonary nodules. World J Surg Oncol 2012;10:25.
5. Maffione AM, Grassetto G, Rampin L, Chondrogiannis S, Marzola MC, Ambrosini V, *et al*. Molecular imaging of pulmonary nodules. AJR Am J Roentgenol 2014;202:W217-23.
6. Edey AJ, Hansell DM. Incidentally detected small pulmonary nodules on CT. Clin Radiol 2009;64:872-84.
7. Kang J, Litmanovich D, Bankier AA, Boiselle PM, Eisenberg RL. Manifestations of systemic diseases on thoracic imaging. Curr Probl Diagn Radiol 2010;39:247-61.
8. Gomez Herrero H, Arraiza Sarasa M, Rubio Marco I, Garcia de Eulate Martin-Moro I. Pulmonary rheumatoid nodules: Presentation, methods, diagnosis and progression in reference to 5 cases. Reumatol Clin 2012;8:212-5.
9. Thomas JW, Staerkel GA, Whitman GJ. Pulmonary hamartoma. AJR Am J Roentgenol 1999;172:1643.
10. Gaerte SC, Meyer CA, Winer-Muram HT, Tarver RD, Conces DJ Jr. Fat-containing lesions of the chest. Radiographics 2002;22 Spec No:S61-78.

11. Cardillo G, Facciolo F, Cavazzana AO, Capece G, Gasparri R, Martelli M. Localized (solitary) fibrous tumors of the pleura: An analysis of 55 patients. Ann Thorac Surg 2000;70:1808-12.
12. Prabhakar HB, Rabinowitz CB, Gibbons FK, O'Donnell WJ, Shepard JA, Aquino SL. Imaging features of sarcoidosis on MDCT, FDG PET, and PET/CT. AJR Am J Roentgenol 2008;190(3 Suppl):S1-6.
13. Chong S, Lee KS, Chung MJ, Han J, Kwon OJ, Kim TS. Pneumoconiosis: Comparison of imaging and pathologic findings. Radiographics 2006;26:59-77.
14. Jedynak AR. Imaging in silicosis and coal worker pneumoconiosis. Medscape 2014.
15. Bankoff MS, McEniff NJ, Bhadelia RA, Garcia-Moliner M, Daly BD. Prevalence of pathologically proven intrapulmonary lymph nodes and their appearance on CT. AJR Am J Roentgenol 1996;167:629-30.
16. Sykes AM, Swensen SJ, Tazelaar HD, Jung SH. Computed tomography of benign intrapulmonary lymph nodes: Retrospective comparison with sarcoma metastases. Mayo Clin Proc 2002;77:329-33.
17. Tanaka N, Kim JS, Newell JD, Brown KK, Cool CD, Meehan R, *et al*. Rheumatoid arthritis-related lung diseases: CT findings. Radiology 2004;232:81-91.
18. Frazier AA, Galvin JR, Franks TJ, Rosado-De-Christenson ML. From the archives of the AFIP: Pulmonary vasculature: Hypertension and infarction. Radiographics 2000;20:491-524.
19. He H, Stein MW, Zalta B, Haramati LB. Pulmonary infarction: Spectrum of findings on multidetector helical CT. J Thorac Imaging 2006;21:1-7.
20. Wilson AG, Joseph AE, Butland RJ. The radiology of aseptic cavitation in pulmonary infarction. Clin Radiol 1986;37:327-33.
21. Martinez F, Chung JH, Digumarthy SR, Kanne JP, Abbott GF, Shepard JA, *et al*. Common and uncommon manifestations of Wegener granulomatosis at chest CT: Radiologic-pathologic correlation. Radiographics 2012;32:51-69.
22. Ananthakrishnan L, Sharma N, Kanne JP. Wegener's granulomatosis in the chest: High-resolution CT findings. AJR Am J Roentgenol 2009;192:676-82.
23. Truong M, Munden RF, Kemp BL. Localized fibrous tumor of the pleura. AJR Am J Roentgenol 2000;174:42.
24. Thourani VH, Sharma J, Duarte IG, Miller JI Jr. Intrathoracic splenosis. Ann Thorac Surg 2005;80:1934-6.
25. Naylor MF, Karstaedt N, Finck SJ, Burnett OL. Noninvasive methods of diagnosing thoracic splenosis. Ann Thorac Surg 1999;68:243-4.
26. Roach HD, Davies GJ, Attanoos R, Crane M, Adams H, Phillips S. Asbestos: When the dust settles an imaging review of asbestos-related disease. Radiographics 2002;22 Spec No:S167-84.
27. Kim KI, Kim CW, Lee MK, Lee KS, Park CK, Choi SJ, *et al*. Imaging of occupational lung disease. Radiographics 2001;21:1371-91.
28. Feldman DJ. Localized interlobar pleural effusion in heart failure. J Am Med Assoc 1951;146:1408-9.
29. Kuhlman JE, Singha NK. Complex disease of the pleural space: Radiographic and CT evaluation. Radiographics 1997;17:63-79.
30. Alderisio WG. Images in cardiovascular medicine. Vanishing tumor. Circulation 2007;115:e381-2.
31. Hanke R, Kretzschmar R. Round atelectasis. Semin Roentgenol 1980;15:174-82.
32. Partap VA. The comet tail sign. Radiology 1999;213:553-4.
33. McHugh K, Blaquiere RM. CT features of rounded atelectasis. AJR Am J Roentgenol 1989;153:257-60.
34. Molinari F, Bankier AA, Eisenberg RL. Fat-containing lesions in adult thoracic imaging. AJR Am J Roentgenol 2011;197:W795-813.
35. Davila DG, Dunn WF, Tazelaar HD, Pairolero PC. Bronchial carcinoid tumors. Mayo Clin Proc 1993;68:795-803.
36. Jeung MY, Gasser B, Gangi A, Charneau D, Ducroq X, Kessler R, *et al*. Bronchial carcinoid tumors of the thorax: Spectrum of radiologic findings. Radiographics 2002;22:351-65.
37. Jones DY. Bronchogenic cyst. Radiopaedia org. 2004. http://radiopaedia.org/articles/bronchogenic-cyst. [Last accessed on 2014 Sept 15].
38. Yoon YC, Lee KS, Kim TS, Kim J, Shim YM, Han J. Intrapulmonary bronchogenic cyst: CT and pathologic findings in five adult patients. AJR Am J Roentgenol 2002;179:167-70.
39. Lucaya JB, Strife JL. Pediatric Chest Imaging. Chest Imaging in Infants and Children 2nd ed.: Springer Verlag; 2007;1:263-87.
40. Cakmaka DG, Gockunb N, Evrenb E, Saglamc ZA. Bronchocele: Two cases. J Med Cases 2013;4:594-7.
41. Brant WE. Fundamentals of diagnostic radiology. 4th ed. Philadelphia: Lippincott Williams & Wilkins.; 2007;1: 410-35.
42. Martinez S, Heyneman LE, McAdams HP, Rossi SE, Restrepo CS, Eraso A. Mucoid impactions: Finger-in-glove sign and other CT and radiographic features. Radiographics 2008;28:1369-82.
43. Pedrosa I, Saiz A, Arrazola J, Ferreiros J, Pedrosa CS. Hydatid disease: Radiologic and pathologic features and complications. Radiographics 2000;20:795-817.
44. Polat P, Kantarci M, Alper F, Suma S, Koruyucu MB, Okur A. Hydatid disease from head to toe. Radiographics 2003;23:475-94.
45. Terris DG. Thyroid and Parathyroid Diseases, Medical and Surgical Management. New York: Thieme Medical Pub.; 2008;2008:81-89.
46. Jeung MY, Gasser B, Gangi A, Bogorin A, Charneau D, Wihlm JM, *et al*. Imaging of cystic masses of the mediastinum. Radiographics 2002;22 Spec No:S79-93.
47. Wang ZJ, Reddy GP, Gotway MB, Yeh BM, Hetts SW, Higgins CB. CT and MR imaging of pericardial disease. Radiographics 2003;23 Spec No:S167-80.
48. Benveniste MF, Rosado-de-Christenson ML, Sabloff BS, Moran CA, Swisher SG, Marom EM. Role of imaging in the diagnosis, staging, and treatment of thymoma. Radiographics 2011;31:1847-61.
49. Santana L, Givica A, Camacho C. Armed Forces Institute of Pathology. Best cases from the AFIP: thymoma. Radiographics 2002;22 Spec No:S95-102.
50. Nagasawa K, Takahashi K, Hayashi T, Aburano T. Ectopic cervical thymoma: MRI findings. AJR Am J Roentgenol 2004;182:262-3.
51. Nishino M, Ashiku SK, Kocher ON, Thurer RL, Boiselle PM, Hatabu H. The thymus: A comprehensive review. Radiographics 2006;26:335-48.
52. Popoveniuc G, Sharma M, Devdhar M, Wexler JA, Carroll NM, Wartofsky L, *et al*. Graves' disease and thymic hyperplasia: The relationship of thymic volume to thyroid function. Thyroid 2010;20:1015-8.
53. Brown LR, Aughenbaugh GL. Masses of the anterior mediastinum: CT and MR imaging. AJR Am J Roentgenol 1991;157:1171-80.
54. Zhang M, Endo M, Adachi S, Kono M. Multilocular thymic cyst: MR findings. AJR Am J Roentgenol 1994;163:479-80.
55. Agarwala R. Extramedullary hematopoiesis (EMH). Available from: http://wwwappliedradiologycom/articles/extramedullary-hematopoiesis-emh. 2006 [Last accessed on 2014 Sept 15].
56. Frederick C, Kidner MD. Calcified Hematoma. JAMA 1917;LXVIII:177-80.
57. Hata Y, Sakamoto S, Shiraga N, Sato K, Sato F, Otsuka H, *et al*. A case of chronic expanding hematoma resulting in fatal hemoptysis. J Thorac Dis 2012;4:508-11.
58. Sato M, Kosaka S, Takahashi T. Life threatening chronic expanding hematoma of the thorax. J Cardiovasc Surg (Torino) 2004;45:511-4.

How to cite this article: Suut S, Al-Ani Z, Allen C, Rajiah P, De, AL-Harbi A, *et al*. Pictorial essay of radiological features of benign intrathoracic masses. Ann Thorac Med 2015;10:231-42.

Source of Support: Nil, **Conflicts of interest:** None declared.